F.D. from N.A.E., Bedford.

R. & M. No. 2941
(ARC 14,701)
A.R.C. Technical Report

MINISTRY OF SUPPLY

AERONAUTICAL RESEARCH COUNCIL
REPORTS AND MEMORANDA

Low-speed Tunnel Model Tests on Tailplane Rolling Moments in Sideslip

By

A. SPENCE, B.Sc., J. W. LEATHERS,
and
D. A. KIRBY, B.Sc.(Eng.)

LONDON: HER MAJESTY'S STATIONERY OFFICE
1955
PRICE 5s 6d NET

Low-speed Tunnel Model Tests on Tailplane Rolling Moments in Sideslip

By

A. Spence, B.Sc., J. W. Leathers,
and
D. A. Kirby, B.Sc.(Eng.)

Communicated by the Principal Director of Scientific Research (Air),
Ministry of Supply

Reports and Memoranda No. 2941*
October, 1951

Summary.—To provide data for stressing purposes, measurements have been made of the effect of sideslip on the rolling moment on a 41·5-deg swept-back tailplane mounted at three heights on the fin of a $\frac{1}{5}$th scale model of a single jet aircraft with a 40-deg swept-back wing. Incidence and tailplane setting were varied, and the effects of rudder deflection were obtained with the tailplane at the top of the fin. Brief results on a delta aircraft model with a delta tailplane at the top of the fin are also included.

(*a*) At zero tailplane lift, for tail heights, 0·31, 0·62 and 0·99 times the fin height external to the body, the values of $(-l_{v\,\mathrm{tail}})$ are 0·111, 0·172 and 0·199 respectively. These values are increased slightly by increase of incidence.

(*b*) The variation with tailplane lift is as estimated for the tailplane alone.

(*c*) Deflecting the rudder changes the rolling moment on the high tailplane in proportion to the change of side force on the fin and rudder. A smaller effect would be expected on lower tailplanes where the flow round the body contributes more to the rolling moment.

---

1. *Introduction.*—Some low-speed tunnel tests have been made to find the rolling moments due to sideslip on a tailplane mounted at three heights on the fin of a single-jet fighter model with swept-back wing and tail surfaces.

Values of the rolling moment on the tailplane were obtained from measurements of the bending moment on the starboard half of the tailplane about a hinge just outside the fin. In order to separate the effects of fin interference, wing and body interference and tailplane lift, a range of incidence and tail-setting were used for each of three tailplane heights. In addition, the effect of rudder deflection was measured with the tailplane at the top of the fin.

The results of a brief test on a delta wing aircraft with a delta tailplane on top of a swept-back fin are also included in this note.

2. *Details of Models and Tests.*—A $\frac{1}{5}$th scale model of a single-jet fighter was used for the main tests. A general arrangement of this is given in Fig. 1 and details in Table 1. No ducts were represented and the rear exit was blocked with a fairly bluff rounded fairing. The sweepback of the wing quarter-chord line was 40 deg, the fin 60 deg and the tailplane 41·5 deg. The three positions of the tailplane are shown in Fig. 2. The heights, measured from the fin root quarter-chord point, were 0·99, 0·62 and 0·31 times the fin height. The high and low positions were based on actual designs for a current aircraft. The tail arm was allowed to vary since it was not of particular importance in the present tests.

The starboard side of the tailplane outboard of 8·4 per cent semi-span was carried on free hinges, the hinge-line being along wind and on the chord line. The gap between the fixed and free parts of the tailplane was about 0·05 inches though half of this was blocked by parts of the

* R.A.E. Tech. Note Aero. 2123, received 4th March, 1952.

hinge system. A complete tailplane hinged on its centre-line was also tested in the high position. In this case the clearance between the top of the fin and the lower surface of the tailplane was made as small as possible.

Bending or rolling moments were obtained by measuring the tension in a wire from the tailplane to an auxiliary balance ; zero tailplane dihedral was indicated by the position of a beam of light reflected by a small concave mirror let into the surface of the tailplane. The relation between the rolling moments on the complete tailplane and the bending moments on the part tailplane in the high position was used to transfer from bending moments to rolling moments for the other tailplane positions where it was not possible to use a complete tailplane. From the results at 2·5 deg and 5 deg sideslip, it was found necessary to multiply the difference of the bending moments at positive and negative sideslip by a constant factor of 1·20 to give agreement with the rolling moments on the complete tailplane. The agreement thus obtained is shown in Table 3, which also shows that a factor of about 1·3 would be needed at 10 deg sideslip. This increased factor is a result of the rapid fall in the bending moment at $\beta = -10$ deg (Fig. 3). The bending moment curves for the lower tailplane positions are much straighter in this region and for this reason the factor of 1·20 has been used throughout.

In addition to the measurements on the tailplanes, overall forces and moments were measured on the model with and without fin and tailplane. For these tests the hinged part of the tailplane was locked, the gap was sealed and the auxiliary balance attachments were removed.

A summary of the conditions used and of the measurements made is given in the following table. In each condition, readings were taken over the range $\beta = 0$ deg, $\pm$ 2·5 deg, $\pm$ 5 deg, and $\pm$ 10 deg.

Condition	α (deg)	η_T (deg)	ζ (deg)	Bending or rolling moments on tailplane	Overall forces and moments
1 No fin or tailplane	1·1, 5·3	—	—	—	Laterals
2 With fin, no tailplane	1·1, 5·3	—	0	—	All six
	2·75	—	0	—	C_m, C_l
3 With fin and high tailplane, centre hinge	1·1	−1·05	0	Rolling	—
		+1·85	0	,,	—
	2·75	−1·0	0	,,	—
	5·3	−0·9	0	,,	—
		+2·0	0	,,	—
4 With fin and high tailplane, hinge at $0{\cdot}084b_T/2$	1·1	−4·3	0	Bending	C_m, C_l
		−1·3	0, $\pm 7\frac{1}{2}$, ± 15	,,	All six at $\zeta = 0°$. Laterals at $\zeta = \pm 15°$
		+1·4	0	,,	C_m, C_l
	2·75	−1·25	0	,,	C_m, C_l
	5·3	−4·15	0	,,	C_m, C_l
		−1·15	0	,,	All six
		+1·55	0	,,	C_m, C_l
5 With fin and mid tailplane, hinge at $0{\cdot}084b_T/2$	1·1	−4·2	0	Bending	C_m, C_l, C_Y
		−1·05	0	,,	All six
		+1·55	0	,,	C_m, C_l
	5·3	−4·05	0	,,	C_m, C_l
		−0·9	0	,,	All six
		+1·7	0	,,	C_m, C_l, C_Y
6 With fin and low tailplane, hinge at $0{\cdot}084b_T/2$	1·1	−4·0	0	Bending	C_m, C_l, C_Y
		−0·95	0	,,	All six
		+1·9	0	,,	C_m, C_l
	5·3	−3·85	0	,,	C_m, C_l
		−0·8	0	,,	All six
		+2·05	0	,,	C_m, C_l, C_Y

For convenience in use, the results have been interpolated to tailplane settings of -4 deg, -1 deg and $+2$ deg throughout this note. The bending and rolling moments on the tailplane are expressed as coefficients C_{BT} and C_{lT} respectively, defined by

$$C_{BT} \text{ (or } C_{lT}) = \frac{\text{Bending (or rolling) moment on tailplane}}{\frac{1}{2}\rho V^2 S_T b_T}$$

where S_T, b_T are the gross area and span of the tailplane.

The overall lateral measurements are given in the form of differences caused by the fin or fin and tailplane. The pitching moments have been converted to tailplane lift coefficients C_{LT} using the projected distance along the body from the moment axis to the tailplane quarter-chord point, and neglecting the tailplane drag. This method results in a maximum error of about $0\cdot005$ in tailplane lift coefficient.

On the delta model (Table 1, Fig. 15), measurements of the bending moment on the port side of the tailplane about a hinge at $11\cdot7$ per cent semi-span were made over a range of sideslip at two incidences for only one tailplane setting. For the swept-back tailplane of the main tests, the factor of $1\cdot20$ between bending and rolling moments shows that the spanwise centre of pressure was slightly further out than if the loading had been elliptic. The factor corresponding to elliptic loading would have been $1\cdot23$. It has therefore been assumed that the loading on the delta tailplane was elliptic, giving a factor of $1\cdot34$ between rolling and bending moments. (The factor is larger because the hinge-line is further from the centre-line on the delta tailplane than on that of the main tests.)

All the tests were made in the No. 1, $11\frac{1}{2} \times 8\frac{1}{2}$-ft tunnel at the Royal Aircraft Establishment during 1950. The wind speed was 120 ft/sec giving Reynolds numbers based on tailplane mean chord of $0\cdot70 \times 10^6$ for the main tests and $0\cdot73 \times 10^6$ for the delta model.

3. *Results and Discussion.*—3.1. *Effect of Tailplane Height on Tailplane Rolling Moment* (*Tables* 2 *to* 4; *Figs.* 3 *to* 9).—Bending moments for the various tailplane heights are plotted against angle of sideslip in Figs. 3 to 5 and the corresponding tailplane rolling moments are given in Figs. 6 and 7. The rolling moments are nearly linear up to 5 deg of sideslip and the slopes (l_{vT} = slope per radian, K = slope per degree) are plotted in Fig. 8 against the lift coefficient on the tailplane at zero sideslip. Over a range of tailplane lift coefficient from about $+0\cdot1$ to $-0\cdot1$, the variation of l_{vT} with C_{LT} agrees fairly well with the value $dl_{vT}/dC_{LT} = -0\cdot247$ estimated from Ref. 1 for the tailplane alone. This estimated slope is shown chain-dotted in Fig. 8.

The results in Fig. 8 also show that there is a small extra effect of incidence not taken into account by using tailplane lift as the main variable. This effect increases as the tailplane is lowered and is probably caused by the spanwise variation of downwash at the tailplane.

The values of l_{vT} at $\alpha = 1\cdot1$ deg and zero lift on the tailplane are plotted against tailplane height in Fig. 9. An estimate has been made of the contribution of the cross flow round the body at the tailplane position, calculated by the method of Ref. 2. The method assumes that body can be treated as an infinitely long circular cylinder, and the body diameter taken was that of the actual body at the same fore-and-aft position as the tailplane mean quarter-chord point. This body effect is also shown in Fig. 9. It is small when the tailplane is at the top of the fin, but accounts for more than half the total rolling moment on the low tailplane.

3.2. *Effect of Rudder Deflection on Tailplane Rolling Moment* (*Table* 8, *Figs.* 11 *and* 12).—In Table 8 and Fig. 11 the changes of bending moment on the high tailplane are given for $\pm 7\frac{1}{2}$ deg and ± 15 deg rudder angle. These results are converted to tailplane rolling moments in Table 8 which also gives the overall changes in side force due to ± 15 deg rudder angle at 0 deg, 5 deg and 10 deg sideslip. Combining these results $10^3 \Delta C_{lT}$ is plotted against $10^3 \Delta C_Y$ in Fig. 12 for a change of rudder angle from $+15$ deg to -15 deg, showing a reduction in $-l_{vT}$ if rudder is applied to trim the yawing moment. On this model, $-l_{vT}$ would be reduced to 62 per cent of the value with rudder undeflected.

A1

If the rolling moment of the high tailplane at zero tailplane lift depends only on the side force on the fin and rudder (*i.e.*, zero body contribution) then a curve of tailplane rolling moment against side force on the fin and rudder at $C_{LT} = 0$ will lie on the same curve as the results for rudder deflection. Fig. 12 shows that the two curves are very nearly the same.

At lower tailplane positions, when the body effect becomes more important (Fig. 9) the effect of rudder would be a smaller proportion of the total rolling moment on the tailplane.

3.3. *Effects of Sideslip on Pitching Moments and Tailplane Lift* (*Figs.* 13 *and* 14).—Fig. 13 shows the change of pitching moment caused by sideslip for the model without tailplane. No systematic variation with incidence was found and the values plotted are means for $\alpha = 1 \cdot 1$ deg, $2 \cdot 75$ deg and $5 \cdot 3$ deg.

Changes of the tailplane contribution to pitching moment have been used to obtain the effect of sideslip on tailplane lift coefficient for the three tailplane heights (Fig. 14). No systematic variation with either incidence or tailplane setting was found and the results given are means for a range of both these variables. The increase of tailplane lift with sideslip does not vary much with the height of the tailplane.

It is worth noting that the shape of the bending-moment curves (Figs. 3 to 5) shows that sideslip gives less loss of lift on the backward-going half of the tailplane than gain on the forward-going half.

3.4. *Results for Delta Model* (*Tables* 9 *and* 10, *Figs.* 16 *to* 19).—The bending moments and deduced rolling moments on the delta model tailplane are shown in Figs. 16 and 17 respectively. The values of l_{vT} and K are

α (deg)	C_{LT}	l_{vT}	K
0·4	−0·08	−0·187	−0·0033
3·6	+0·025	−0·206	−0·0036

The variation of l_{vT} with tailplane lift is the same as would be expected on the tailplane alone (Ref. 1 gives $dl_{vT}/dC_{LT} = -0 \cdot 18$). The value of $l_{vT} = -0 \cdot 201$ interpolated at zero tailplane lift compares with $-0 \cdot 199$ for the high tailplane of the main tests at the lower incidence.

The effect of sideslip on pitching moment without tailplane is shown in Fig. 18, and on tailplane lift coefficient in Fig. 19. The curves agree very closely with those for the model of the main tests given in Figs. 13 and 14 respectively.

LIST OF SYMBOLS

S_T	Area of tailplane
b_T	Span of tailplane
C_{BT}	Tailplane bending moment $\div \frac{1}{2}\rho V^2 S_T b_T$
C_{lT}	Tailplane rolling moment $\div \frac{1}{2}\rho V^2 S_T b_T$
C_{LT}	Tailplane lift coefficient
l_{vT}	Slope $dC_{lT}/d\beta$ per radian
K	Slope $dC_{lT}/d\beta$ per degree

REFERENCES

No.	*Author*	*Title, etc.*
1	I. Levačić	Rolling moment due to sideslip. Part II: The effect of sweepback and plan form. R.A.E. Report Aero. 2092. A.R.C. 9278. November, 1945. (Unpublished.)
2	I. Levačić	Rolling moment due to sideslip. Part III: The effects of wing body arrangement and tail unit. R.A.E. Report Aero. 2139, A.R.C. 9987. July, 1946. (Unpublished.)

TABLE 1

Details of Models

	Main Test Model	Delta Model
Wing		
Area S	13·84 sq. ft	18·20 sq ft
Span b	6·70 ft	7·287 ft
Mean chord $\bar{c} = S/b$	2·066 ft	2·5 ft
Aspect ratio A	3·24	2·92
Chord at centre-line	2·946 ft	4·57 ft
Chord at tip	1·217 ft	0·457 ft
Sweepback	40 deg (quarter chord)	48·5 deg (leading edge)
Dihedral	−0·8 deg	0 deg
Moment Axis		
Aft of leading edge at centre-line	2·048 ft	2·45 ft
Aft of leading edge of S.M.C.	$0·305\bar{c}$	
Distance below wing chord at centre-line	0·115 ft	
Fuselage		
Wing-body angle	1·5 deg	0 deg
Intersection of wing chord at centre-line and fuselage datum, aft of nose	3·55 ft	
Fuselage diameter at intersection	0·875 ft	
Tailplane		
Area S_T	2·05 sq ft	2·34 sq ft
Span b_T	2·20 ft	2·43 ft
Mean chord $c_T = S_T/b_T$	0·933 ft	0·963 ft
Taper ratio	1·71 : 1	5 : 1
Sweepback of quarter-chord line	41·5 deg	42·8 deg
Arm (moment axis to mean quarter-chord point) l_T		
High tailplane	4·098 ft	3·057 ft
Mid tailplane	3·490 ft	
Low tailplane	3·031 ft	
Height of tailplane above fin root quarter-chord		
High tailplane	0·829 ft	1·17 ft
Mid tailplane	0·521 ft	
Low tailplane	0·260 ft	
Distance of mean quarter-chord point aft of centre-line chord leading edge	0·738 ft	
Fin and Rudder		
Fin area (external to fuselage) S_F	1·296 sq ft	1·95 sq ft
Arm (moment axis to mean quarter-chord point) l_F	2·94 ft	2·02 ft
Rudder area aft of hinge-line	0·267 sq ft	
Aspect ratio	0·54	0·70
Sweepback of quarter-chord line (fin above fuselage)	60 deg	47·6 deg

TABLE 2

Bending Moments on Half Tailplane

Hinged at $0 \cdot 084 \frac{b_T}{2}$

Rudder undeflected

β (deg)	$10^3 C_{BT}$						
	High tailplane			Mid tailplane		Low tailplane	
	$\alpha = 1 \cdot 1°$	$\alpha = 2 \cdot 75°$	$\alpha = 5 \cdot 3°$	$\alpha = 1 \cdot 1°$	$\alpha = 5 \cdot 3°$	$\alpha = 1 \cdot 1°$	$\alpha = 5 \cdot 3°$
	$\eta_T = 2°$						
10	−25·6		−39·6	−19·5	−32·0	−13·0	−23·4
5	−16·3		−29·1	−12·0	−22·6	−7·4	−16·8
2·5	−12·0		−24·0	−8·1	−18·5	−4·7	−13·8
0	−7·8		−18·2	−5·0	−14·3	−2·7	−10·9
−2·5	−4·2		−13·2	−1·3	−10·5	−0·7	−8·5
−5	−0·8		−9·8	+0·7	−7·5	+1·0	−6·1
−10	+3·2		−4·4	+4·6	−2·8	+3·8	−3·0
	$\eta_T = -1°$						
10	−10·0	−15·5	−23·1	−6·2	−18·0	1·7	−8·5
5	−2·0	−7·3	−13·5	+1·7	−9·1	7·2	−2·6
2·5	+1·8	−3·0	−9·1	5·1	−5·0	8·9	+0·3
0	5·3	+1·2	−5·2	8·2	−1·8	10·5	2·3
−2·5	8·5	4·3	−1·3	10·0	+1·5	12·0	4·5
−5	11·1	7·0	+1·9	12·7	4·5	13·5	6·3
−10	+11·8	+8·3	+4·0	+15·0	+7·1	15·8	+8·4
	$\eta_T = -4°$						
10	5·8		−8·4	8·2	−3·7	16·7	6·4
5	12·6		+0·5	15·3	+4·5	21·9	12·1
2·5	15·9		4·5	18·5	8·0	23·8	14·5
0	18·7		7·6	21·1	10·9	25·2	16·6
2·5	21·4		10·6	22·8	13·5	25·7	17·7
−5	23·6		13·5	24·6	15·5	26·3	18·7
−10	23·6		+13·4	26·9	+17·0	28·6	20·2

TABLE 3

Tailplane Rolling Moments, Rudder Undeflected

Condition	β (deg)	$10^3 C_{l_T}$ $\alpha = 1 \cdot 1°$	$\alpha = 2 \cdot 75°$	$\alpha = 5 \cdot 3°$
		$\eta_T = 2°$		
High tail	2·5	−10·0		−11·5
	5	−19·0		−22·9
	10	−36·3		−43·0
		$\eta_T = -1°$		
Centre hinge	2·5	−7·6	−8·4	−10·0
	5	−15·2	−16·8	−18·8
	10	−29·2	−31·4	−36·2
		$\eta_T = 2°$		
High tail	2·5	−9·4		−13·0
	5	−18·6		−23·1
	10	−34·6		−42·2
		$\eta_T = -1°$		
Hinge at 0·084 $b_T/2$	2·5	−8·0	−8·8	−9·4
	5	−15·7	−17·2	−18·5
	10	−26·2	−28·6	−32·5
		$\eta_T = -4°$		
	2·5	−6·6		−7·3
	5	−13·2		−15·6
	10	−21·4		−26·2
		$\eta_T = 2°$		
Mid tail	2·5	−8·2		−9·6
	5	−15·2		−18·1
	10	−28·9		−35·0
		$\eta_T = -1°$		
Hinge at 0·084 $b_T/2$	2·5	−5·9		−7·8
	5	−13·2		−16·3
	10	−25·4		−30·2
		$\eta_T = -4°$		
	2·5	−5·2		−6·6
	5	−11·2		−13·2
	10	−22·4		−24·8

TABLE 3—*continued*

Tailplane Rolling Moments, Rudder Undeflected

Condition	β (deg)	$10^3 C_{lT}$		
		$\alpha = 1 \cdot 1°$	$\alpha = 2 \cdot 75°$	$\alpha = 5 \cdot 3°$
		$\eta_T = 2°$		
Low tail	2·5	−4·8		−6·4
	5	−10·1		−12·8
	10	−20·2		−24·4
		$\eta_T = -1°$		
Hinge at 0·084 $b_T/2$	2·5	−3·7		−5·0
	5	−7·6		−10·8
	10	−16·9		−20·1
		$\eta_T = -4°$		
	2·5	−2·3		−3·8
	5	−5·2		−7·9
	10	−14·3		−16·6

TABLE 4

Tailplane Lift Coefficients

η_T (deg)	β (deg)	C_{LT}						
		High tailplane			Mid tailplane		Low tailplane	
		$\alpha = 1 \cdot 1°$	$\alpha = 2 \cdot 75°$	$\alpha = 5 \cdot 3°$	$\alpha = 1 \cdot 1°$	$\alpha = 5 \cdot 3°$	$\alpha = 1 \cdot 1°$	$\alpha = 5 \cdot 3°$
2	10	0·121		0·239	0·065	0·178	0·050	0·144
	5	0·070			0·032	0·140	0·024	0·118
	2·5	0·060			0·034	0·139	0·020	0·111
	0	0·058		0·172	0·034	0·136	0·023	0·110
	−2·5	0·055			0·036	0·140	0·022	0·116
	−5	0·057			0·040	0·144	0·029	0·124
	−10	0·098		0·233	0·081	0·192	0·055	0·156
−1	10	−0·014	+0·031	0·101	−0·066	0·044	−0·086	+0·009
	5	−0·065	−0·019	0·051	−0·101	0·007	−0·111	−0·021
	2·5	−0·075	−0·030	0·039	−0·105	0·002	−0·113	−0·025
	0	−0·077	−0·033	0·035	−0·106	0	−0·117	−0·027
	−2·5	−0·081	−0·035	0·035	−0·105	0	−0·116	−0·022
	−5	−0·078	−0·032	0·038	−0·098	0·007	−0·103	−0·018
	−10	−0·052	+0·005	0·092	−0·061	0·054	−0·075	+0·037
−4	10	−0·160		−0·029	−0·198	−0·084	−0·237	−0·135
	5	−0·212			−0·233	−0·119	−0·259	−0·164
	2·5	−0·220			−0·235	−0·126	−0·264	−0·165
	0	−0·223		−0·103	−0·237	−0·127	−0·266	−0·166
	−2·5	−0·224			−0·237	−0·124	−0·262	−0·162
	−5	−0·221			−0·229	−0·118	−0·252	−0·154
	−10	−0·173		−0·041	−0·191	−0·068	−0·222	−0·116

TABLE 5

Overall Force and Moment Measurements.
No Fin or Tailplane

α (deg)	β (deg)	C_L	C_D	C_m	10^3C_n	10^3C_Y	10^3C_l
1·1	10	0·040			−9·47	−20·21	−2·43
	5				−5·46	−6·97	−2·73
	2·5				−2·92	−2·34	−2·70
	0				−0·08	+0·24	−2·60
	−2·5				+2·85	2·87	−2·77
	−5				5·23	7·15	−2·85
	−10				+9·15	+18·75	−3·34
5·3	10	0·276			−8·62	−22·57	−10·58
	5				−4·96	−6·86	−6·73
	2·5				−2·64	−2·03	−4·14
	0				−0·27	+0·85	−2·07
	−2·5				+2·44	3·60	+0·03
	−5				4·69	8·05	2·11
	−10				+8·53	+22·67	+6·53

TABLE 6

Overall Force and Moment Measurements
With Fin but no Tailplane

α (deg)	β (deg)	C_L	C_D*	C_m	10^3C_n	10^3C_Y	10^3C_l
1·1	10	0·041	0·0190	−0·0178	+6·51	−59·36	−5·35
	5	0·039	0·0125	−0·0110	2·24	−26·39	−3·84
	2·5	0·037	0·0114	−0·0085	1·26	−13·25	−3·36
	0	0·034	0·0107	−0·0073	0·65	−1·91	−2·91
	−2·5	0·037	0·0112	−0·0081	+0·22	+8·81	−2·20
	−5	0·035	0·0123	−0·0095	−0·80	20·95	−1·05
	−10	0·042	0·0184	−0·0158	−4·60	+54·37	+0·52
2·75	10	0·131	0·0130	−0·0148			−9·13
	5			−0·0078			−6·40
	2·5			−0·0058			−4·94
	0			−0·0040			−2·69
	−2·5			−0·0047			−0·82
	−5			−0·0060			+0·81
	−10			−0·0129			+3·57
5·3	10	0·274	0·0290	−0·0121	+7·12	−60·12	−12·72
	5	0·275	0·0219	−0·0057	2·48	−26·41	−7·72
	2·5	0·274	0·0206	−0·0034	1·50	−12·63	−5·25
	0	0·274	0·0207	−0·0026	+0·60	−1·07	−2·73
	−2·5	0·274	0·0206	−0·0026	−0·12	+8·91	+0·18
	−5	0·274	0·0217	−0·0041	−1·06	21·99	2·76
	−10	0·274	0·0282	−0·0095	−4·64	+53·91	+8·64

* C_D is the coefficient of the force along the wind direction

TABLE 7

Changes of Yawing and Rolling Moment and Side Force Caused by Fin or Fin and Tailplane

α (deg)	β (deg)	$10^3 \Delta C_n$			
		With fin no tailplane	High tailplane	Mid tailplane	Low tailplane
1·1	0	0	0	0	0
	2·5	3·4	5·2	4·2	3·6
	5	6·9	10·7	8·1	7·3
	10	14·9	21·0	17·2	15·1
5·3	0	0	0	0	0
	2·5	3·4	5·0	4·1	3·4
	5	6·6	10·2	7·8	7·0
	10	14·5	18·9	15·7	14·0

α (deg)	β (deg)	$10^3 \Delta C_l$			
		With fin no tailplane	High tailplane	Mid tailplane	Low tailplane
1·1	0	0	0	0	0
	2·5	−0·6	−1·6	−0·8	−0·6
	5	−1·5	−3·1	−1·9	−1·2
	10	−3·4	−6·1	−4·3	−3·7
5·3	0	0	0	0	0
	2·5	−0·6	−1·6	−1·0	−0·8
	5	−0·8	−2·4	−2·1	−1·3
	10	−2·1	−4·7	−4·5	−3·0

α (deg)	β (deg)	$10^3 \Delta C_Y$							
		With fin no tailplane	High tailplane	Mid tailplane			Low tailplane		
			$\eta_T = 1°$	$\eta_T = 2°$	$\eta_T = -1°$	$\eta_T = -4°$	$\eta_T = 2°$	$\eta_T = -1°$	$\eta_T = -4°$
1·1	0	0	0		0	0		0	0
	2·5	−8·4	−12·5		−10·3	−10·6		−9·3	−9·9
	5	−16·6	−23·6		−20·6	−21·3		−18·6	−19·3
	10	−37·4	−49·3		−45·0	−43·7		−39·6	−39·5
5·3	0	0	0	0	0		0	0	0
	2·5	−8·0	−11·6	−9·9	−11·3		−8·4	−10·0	
	5	−16·7	−23·4	−19·4	−21·5		−18·1	−18·4	
	10	−34·4	−43·9	−37·1	−40·4		−34·2	−35·0	

Notes: (*a*) Changes of yawing moment measured at $\eta_T = -1$ deg

(*b*) Changes of rolling moment are means of $\eta_T = -4$ deg, -1 deg and $+2$ deg

TABLE 8

Effects of Rudder Deflection—Model with High Tailplane, $\alpha = 1 \cdot 1$ deg, $\eta_T = -1$ deg

(*a*) Changes of bending moment on tailplane, hinged at $0 \cdot 084 \frac{b_T}{2}$

β (deg)	$10^3 \Delta C_{BT}$ due to rudder				
	$\zeta = 15°$	$\zeta = 7 \cdot 5°$	$\zeta = 0$	$\zeta = -7 \cdot 5°$	$\zeta = -15°$
10	5·6	2·85	0	−2·85	−7·0
5	6·1	3·05	0	−3·1	−7·55
2·5		3·3	0	−3·3	
0	6·55	3·3	0	−3·25	−7·25
−2·5		3·1	0	−3·1	
−5	5·45	2·75	0	−2·6	−6·3
−10	5·35	2·2	0	−2·2	−5·0

(*b*) Changes of tailplane rolling moment, obtained from bending moment measurements

β (deg)	$10^3 \Delta C_{lT}$ due to rudder				
	$\zeta = 15°$	$\zeta = 7 \cdot 5°$	$\zeta = 0°$	$\zeta = -7 \cdot 5°$	$\zeta = -15°$
10	12·7	6·05	0	−6·05	−14·8
5	14·9	6·8	0	−7·0	−15·6
2·5		7·7	0	−7·7	
0	16·6	7·85	0	−7·85	−16·6
−2·5		7·7	0	−7·7	
−5	15·6	7·0	0	−6·8	−14·9
−10	14·8	6·05	0	−6·05	−12·7

(*c*) Changes of overall yawing moment, side force, and rolling moment

β (deg)	$10^3 \Delta$ due to change $\zeta = +15°$ to $\zeta = -15°$		
	$10^3 \Delta C_n$	$10^3 \Delta C_Y$	$10^3 \Delta C_l$
10	19·4	−35·0	−4·4
5	20·6	−38·0	−5·6
0	22·8	−42·2	−6·1
−5	20·8	−39·7	−5·4
−10	18·7	−35·7	−5·8

Δy_v due to fin, rudder undeflected $= 0 \cdot 135$ and the change in Δy_v due to deflecting the rudder to trim the yawing moment $= 0 \cdot 084$.

TABLE 9

Bending and Rolling Moments on Tailplane of Delta Model, Rudder Undeflected

Condition	β (deg)	$10^3 C_{BT}$	$10^3 C_{lT}$
$\alpha = 0\cdot4°$	6	$-14\cdot9$	$-19\cdot3$
	4	$-12\cdot8$	$-13\cdot3$
$\eta_T = 0°$	2	$-11\cdot0$	$-7\cdot0$
	0	$-8\cdot5$	0
$C_{LT} = -0\cdot08$	-2	$-5\cdot8$	
	-4	$-2\cdot9$	
	-6	$-0\cdot5$	
$\alpha = 3\cdot6°$	6	$-8\cdot2$	$-21\cdot9$
	4	$-6\cdot2$	$-14\cdot7$
$\eta_T = 0\cdot15°$	2	$-4\cdot0$	$-7\cdot5$
	0	$-1\cdot3$	0
$C_{LT} = 0\cdot028$	-2	$+1\cdot6$	
	-4	$4\cdot8$	
	-6	$+8\cdot1$	

C_{BT} is the measured bending-moment coefficient on the port half of the tailplane, about the hinge-line $0\cdot117b_T/2$ from the centre-line.

C_{lT} is the total tailplane rolling-moment coefficient about the centre-line, assuming that the additional loading due to sideslip is elliptic.

TABLE 10

Lift and Pitching Moment without Tailplane, and Tailplane Lift—Delta Model

α (deg)	η_T (deg)	β (deg)	C_L no tailplane	C_m no tailplane	C_{LT}
		6	$0\cdot021$	$-0\cdot0010$	$-0\cdot065$
		4	$0\cdot020$	$+0\cdot0009$	$-0\cdot076$
		2	$0\cdot020$	$0\cdot0021$	$-0\cdot075$
$0\cdot4$	0	0	$0\cdot020$	$0\cdot0020$	$-0\cdot080$
		-2	$0\cdot019$	$0\cdot0015$	$-0\cdot082$
		-4	$0\cdot017$	$+0\cdot0002$	$-0\cdot083$
		-6	$0\cdot018$	$-0\cdot0017$	$-0\cdot079$
		6	$0\cdot192$	$-0\cdot0038$	$0\cdot048$
		4	$0\cdot192$	$-0\cdot0017$	$0\cdot036$
		2	$0\cdot194$	$-0\cdot0010$	$0\cdot032$
$3\cdot6$	$0\cdot15$	0	$0\cdot192$	$-0\cdot0011$	$0\cdot028$
		-2	$0\cdot191$	$-0\cdot0011$	$0\cdot031$
		-4	$0\cdot190$	$-0\cdot0021$	$0\cdot025$
		-6	$0\cdot194$	$-0\cdot0045$	$0\cdot032$

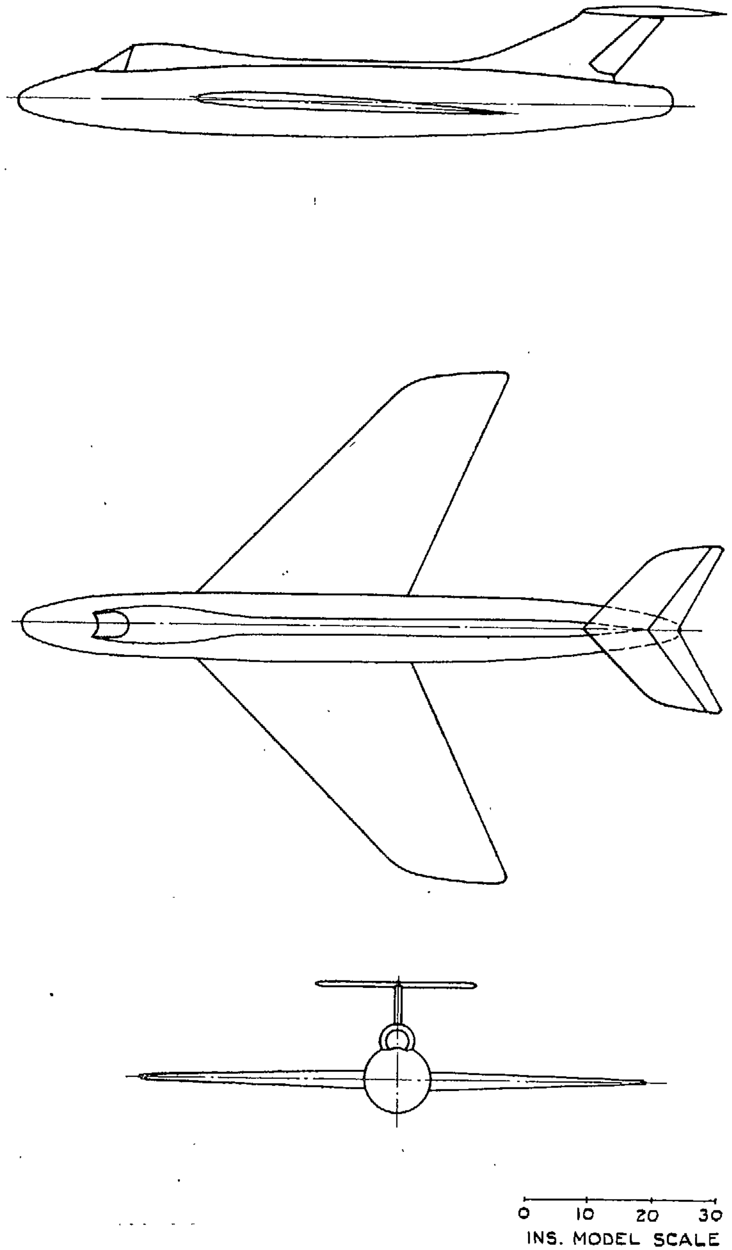

FIG. 1. General arrangement of model showing high tailplane.

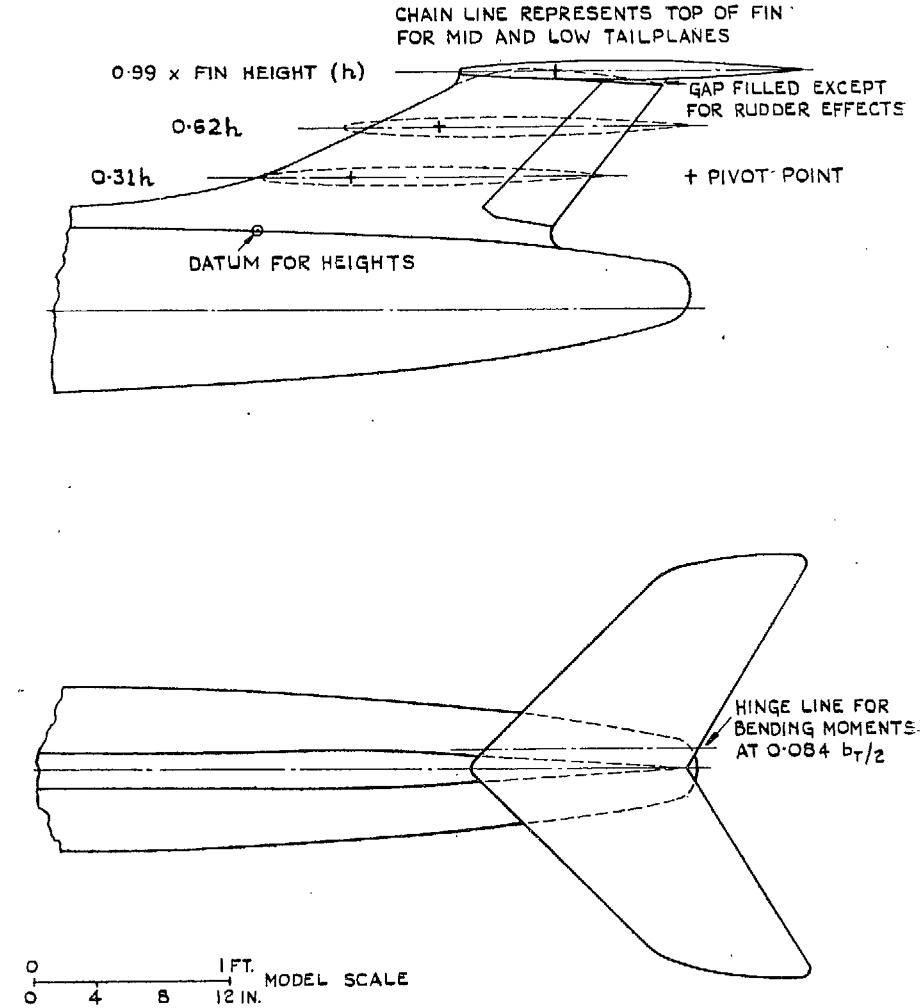

FIG. 2. Details of fin and tailplane positions.

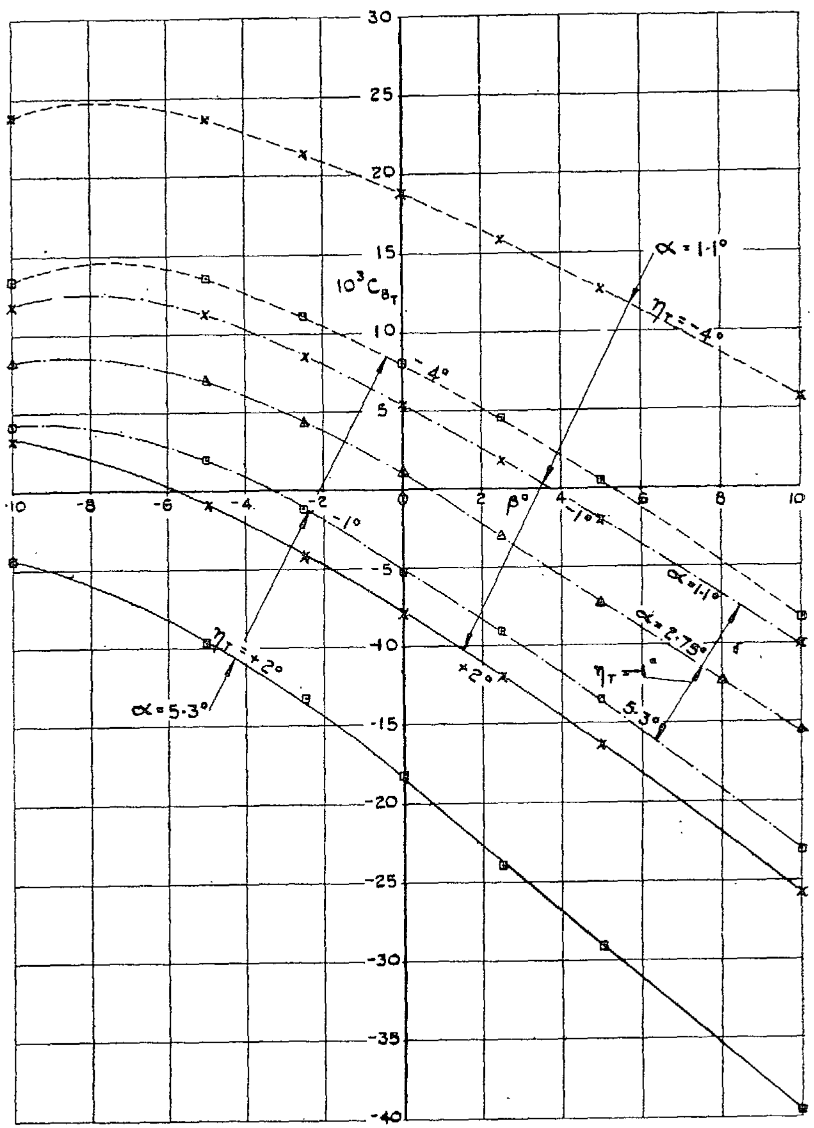

FIG. 3. Bending moments on high tailplane.
Starboard side hinged at $0{\cdot}084\ b_T/2$.

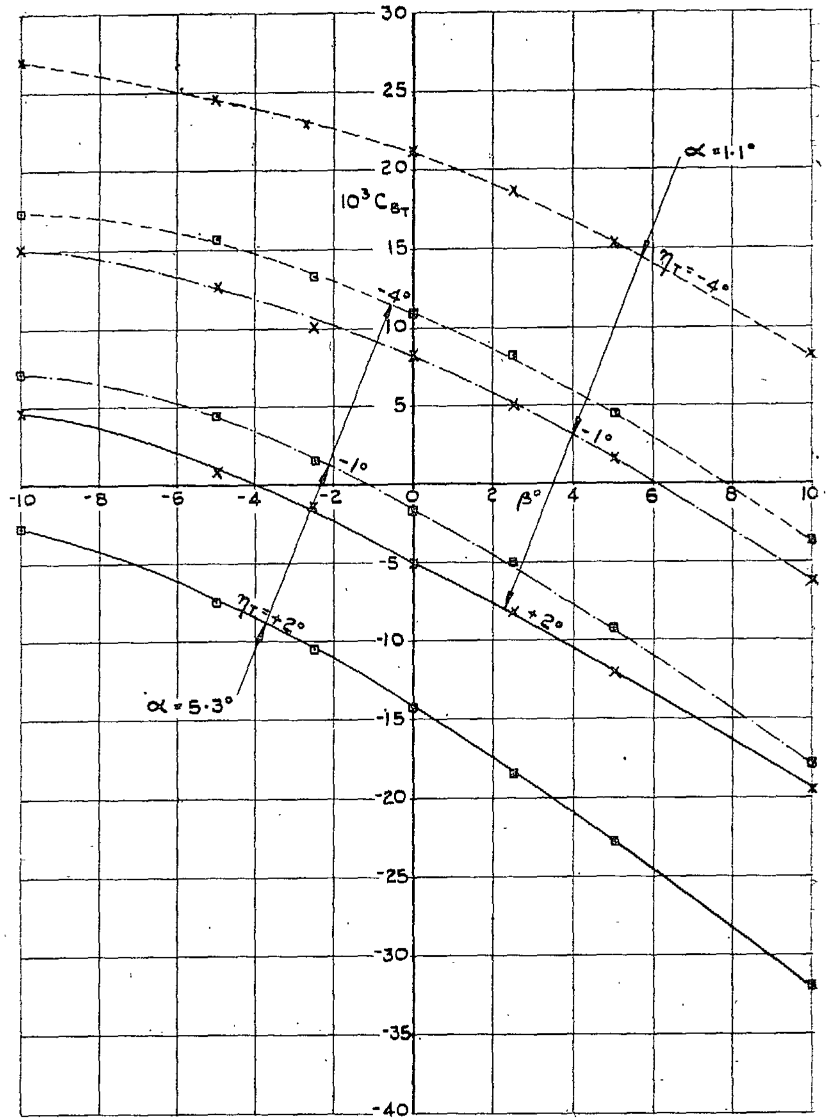

FIG. 4. Bending moments on mid tailplane.
Starboard side hinged at $0{\cdot}084\ b_T/2$.

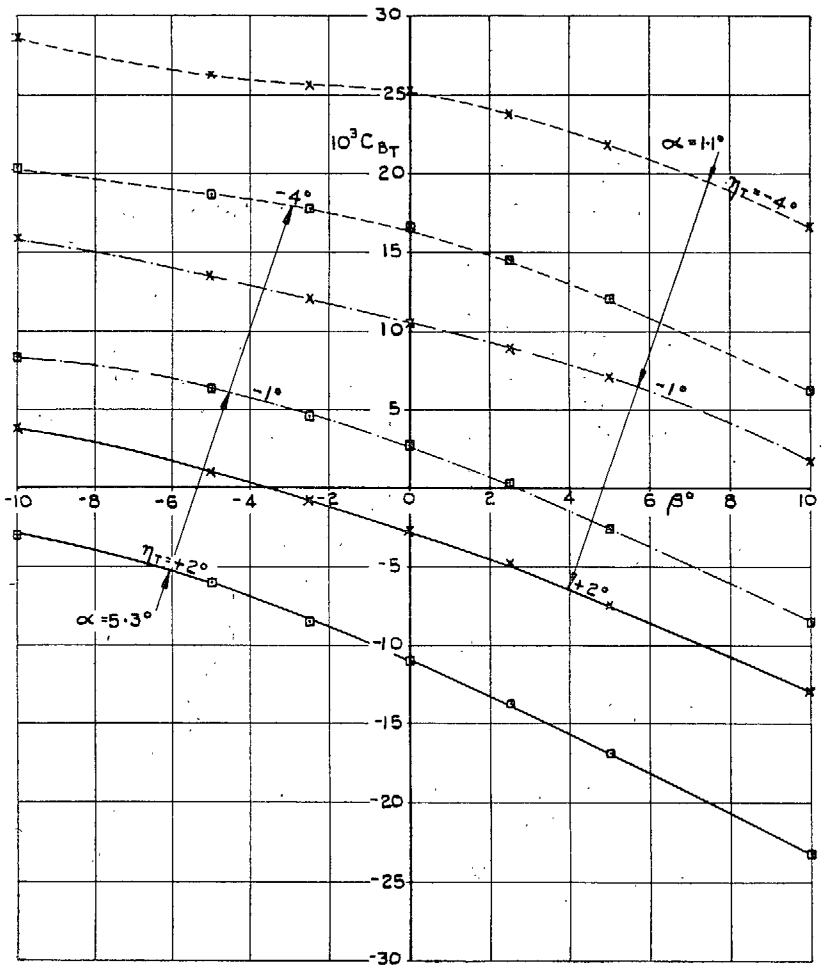

FIG. 5. Bending moments on low tailplane.
Starboard side hinged at $0{\cdot}084 b_T/2$.

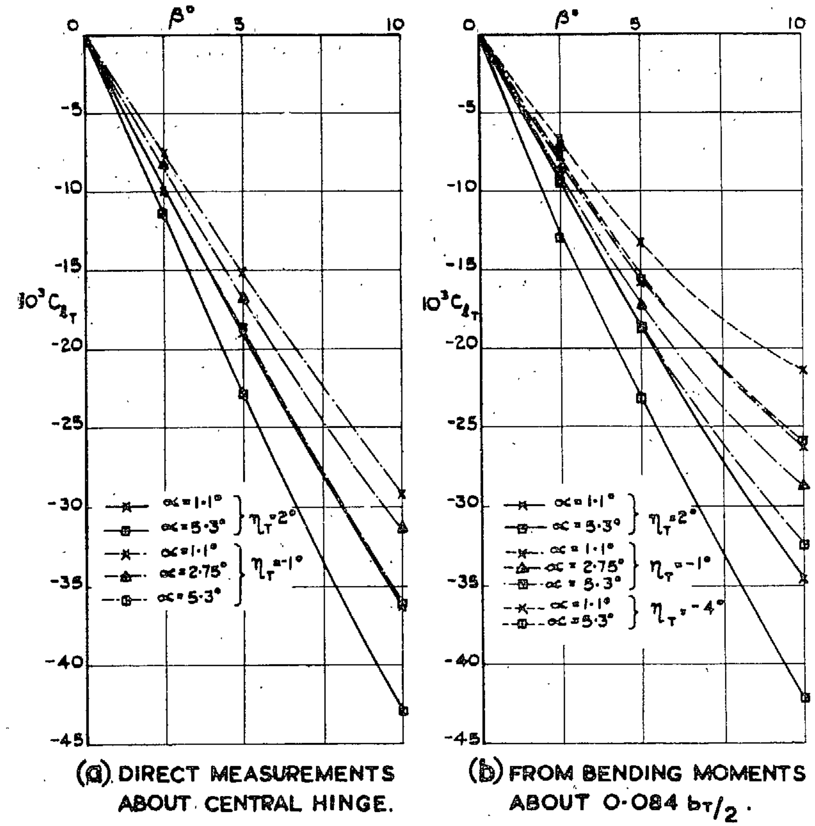

FIGS. 6a and 6b. Rolling moments on high tailplane.

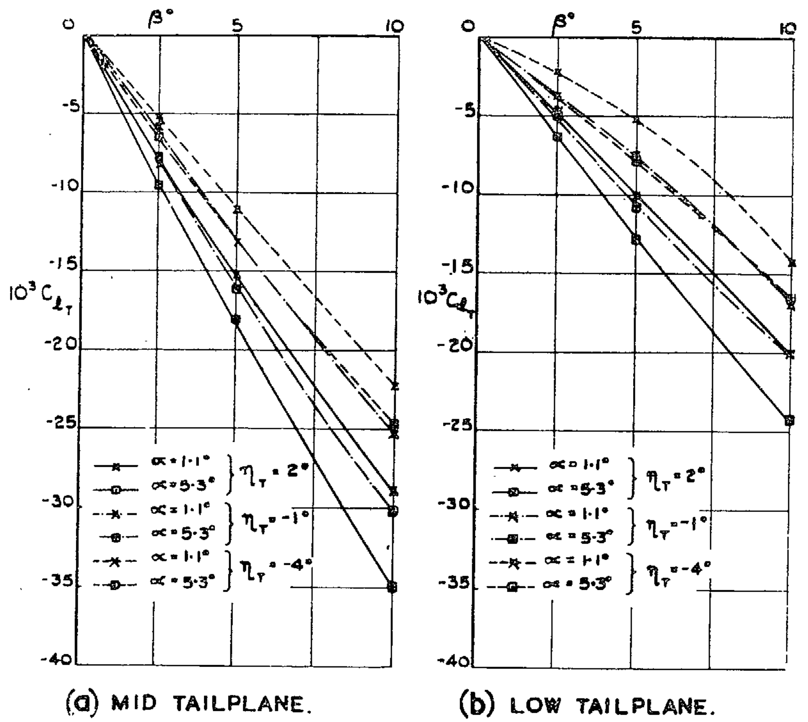

FIGS. 7a and 7b. Rolling moments on mid and low tailplanes.

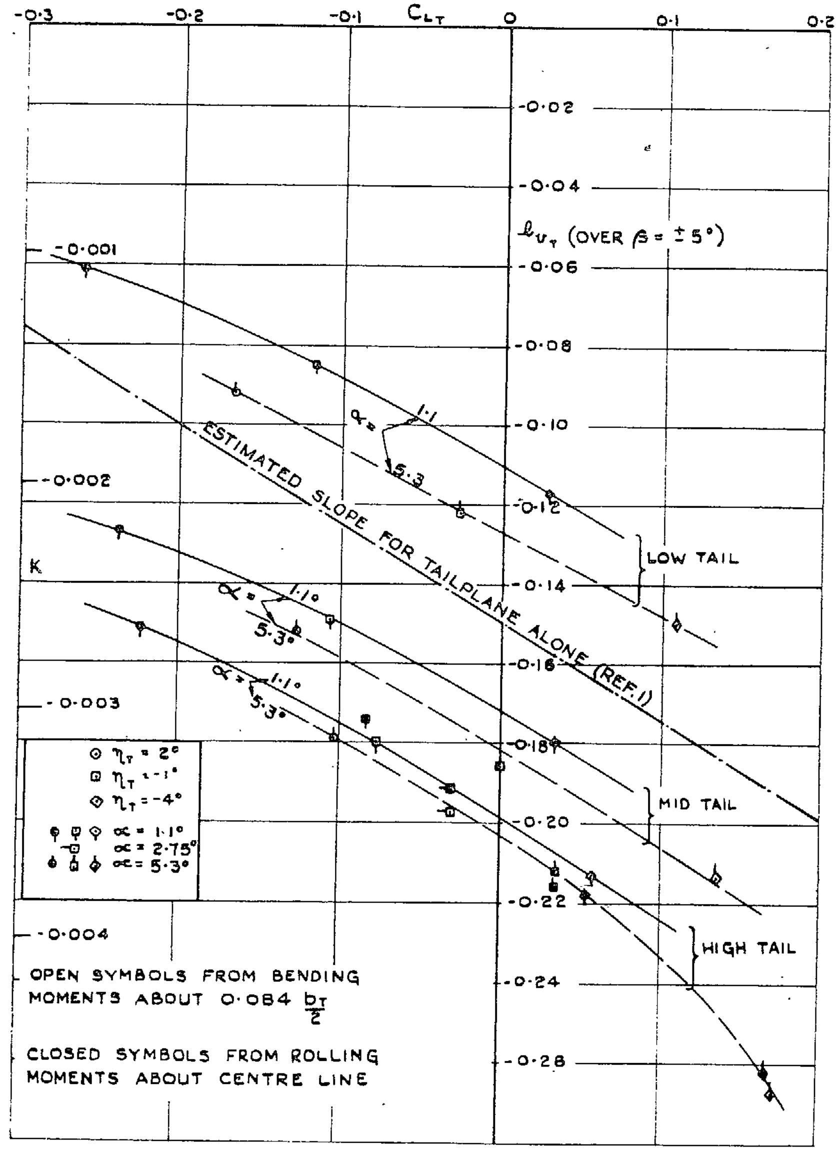

FIG. 8. l_v (tailplane) *vs.* tailplane lift, rudder undeflected.

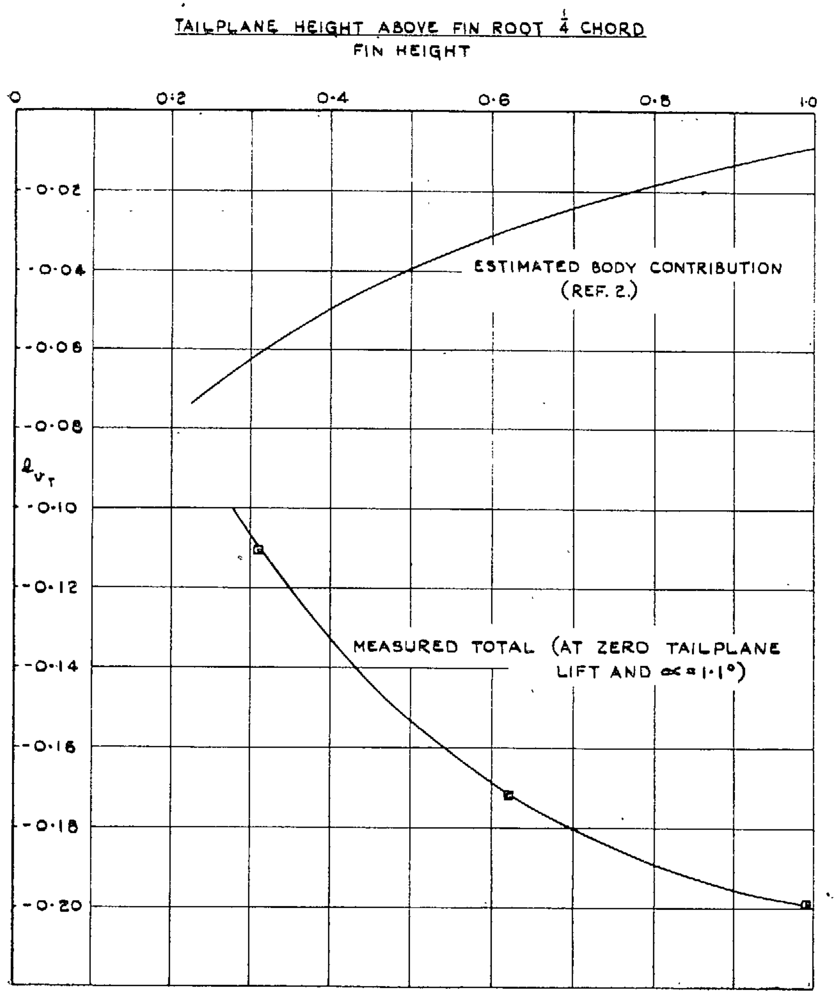

FIG. 9. Effect of tailplane height on tailplane rolling moments.

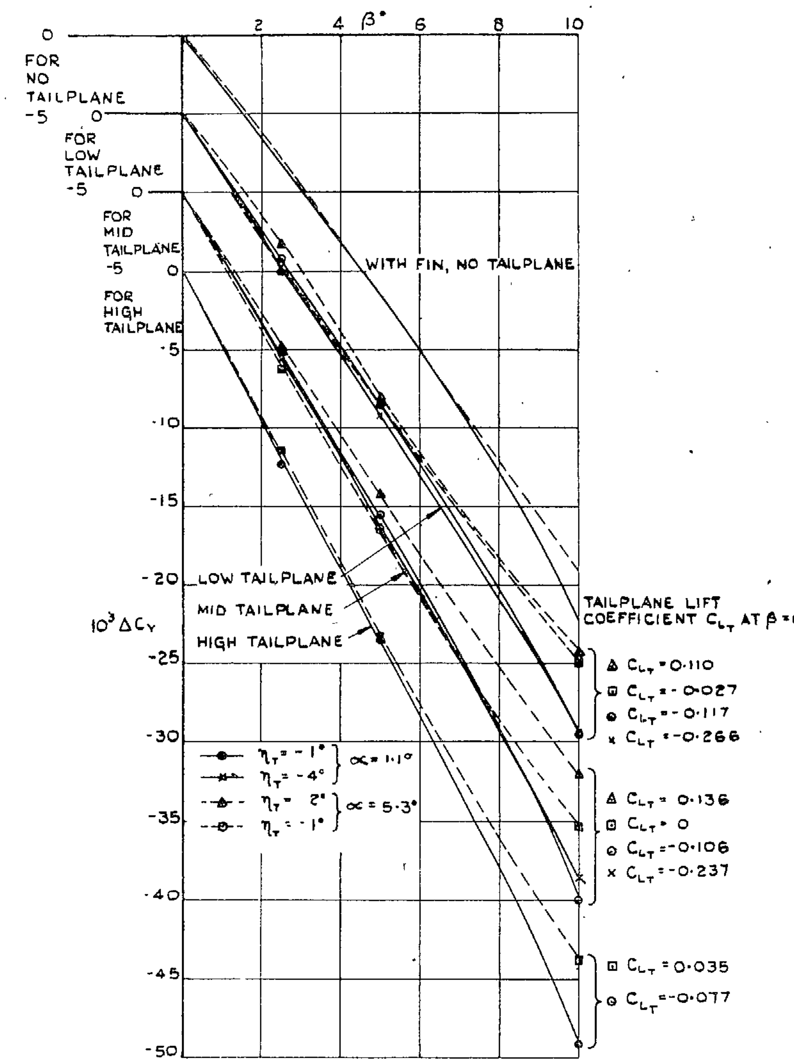

FIG. 10. Changes of side force caused by fin or fin and tailplane.

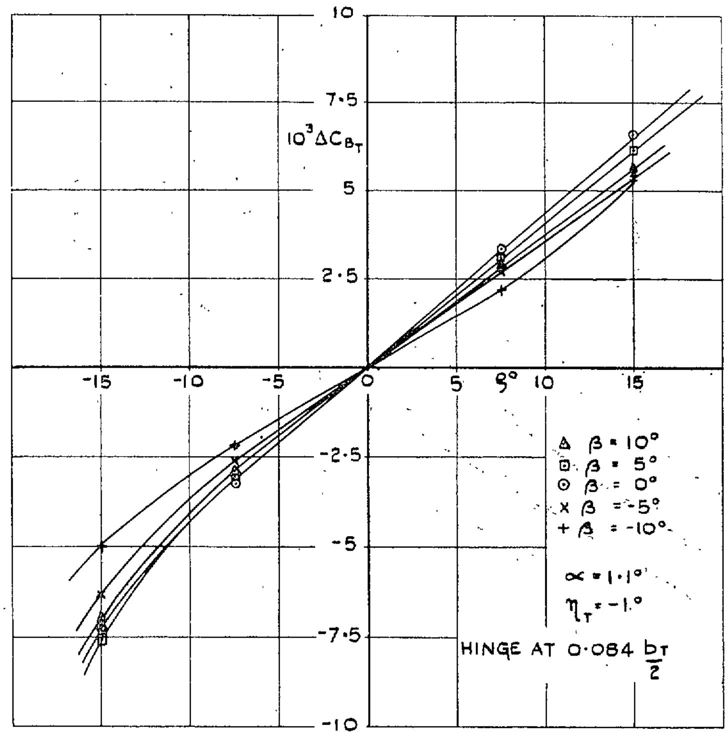

FIG. 11. Change of bending moment with rudder deflection on high tailplane.

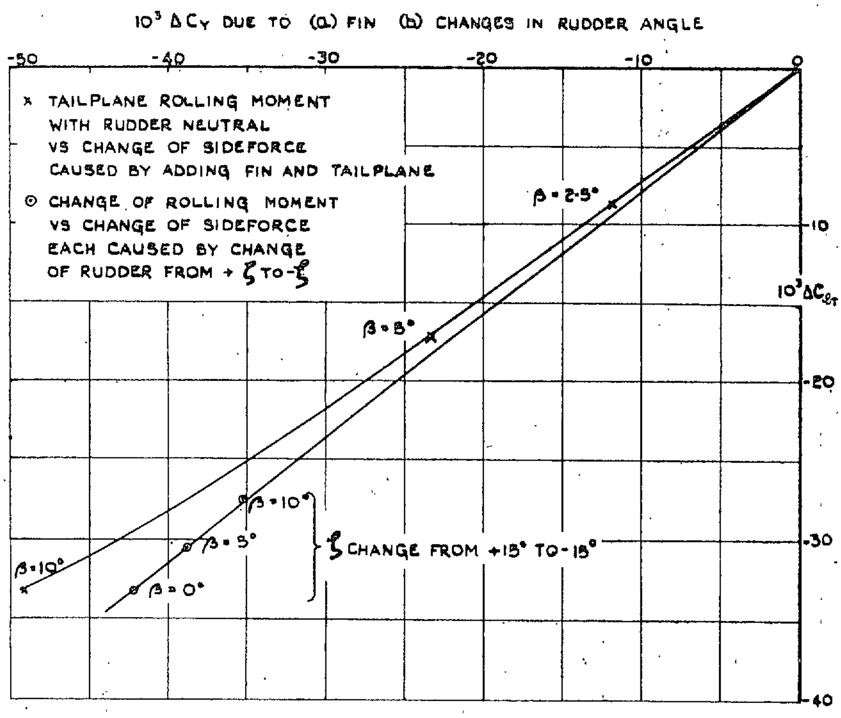

FIG. 12. Effect of rudder deflection on rolling moments of high tailplane.

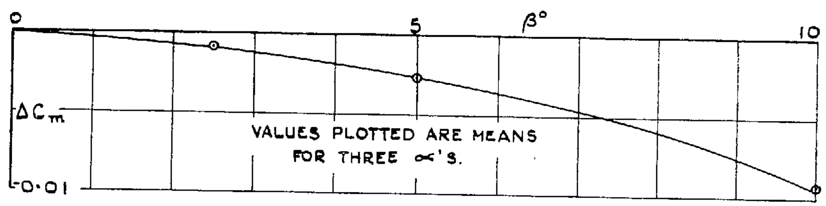

FIG. 13. Pitching moment changes due to sideslip, no tailplane.

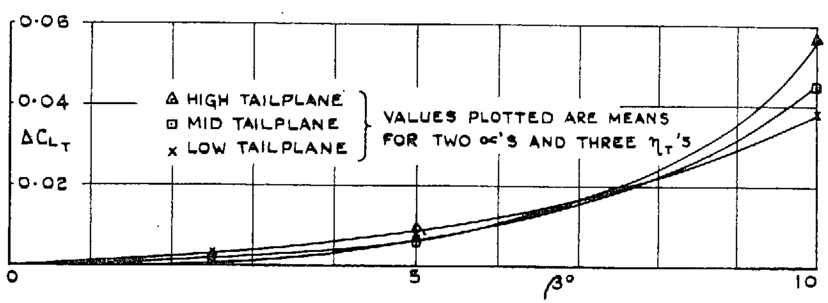

FIG. 14. Tailplane lift changes due to sideslip.

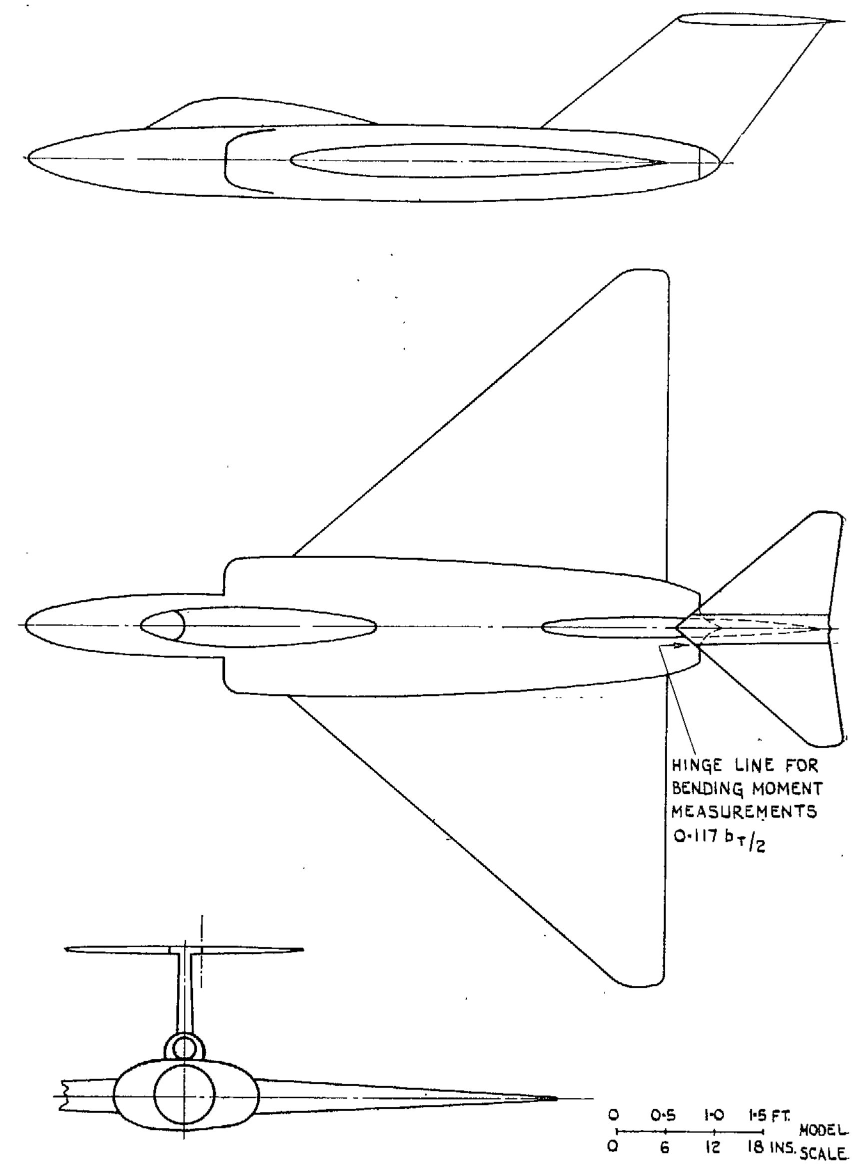

FIG. 15. General arrangement of delta model.

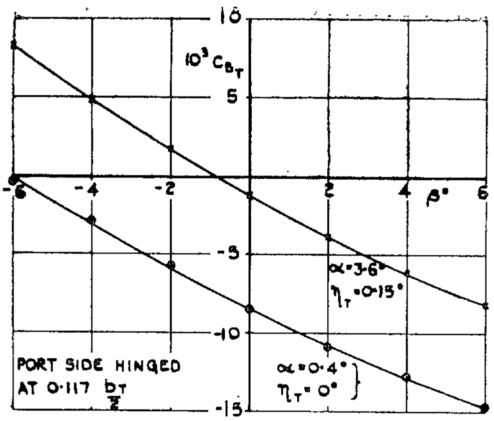

FIG. 16. Tailplane bending moments.

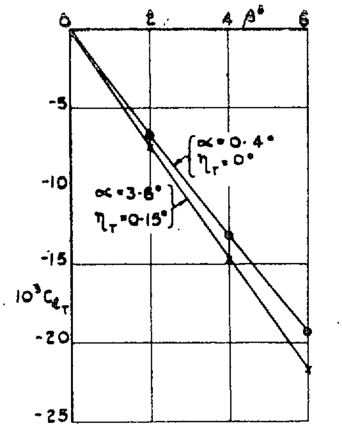

FIG. 17. Tailplane rolling moments.

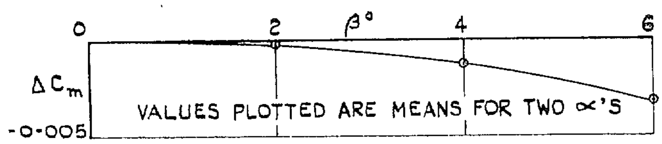

FIG. 18. Pitching moment changes due to sideslip, no tailplane.

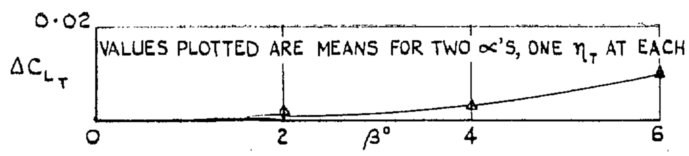

FIG. 19. Tailplane lift changes due to sideslip.

FIGS. 16 to 19. Results on delta model.

J4317 Wt.18/9296 K9 2/55 D&Co. 34/263

PRINTED IN GREAT BRITAIN

Publications of the Aeronautical Research Council

ANNUAL TECHNICAL REPORTS OF THE AERONAUTICAL RESEARCH COUNCIL (BOUND VOLUMES)

1936 Vol. I. Aerodynamics General, Performance, Airscrews, Flutter and Spinning. 40*s.* (41*s.* 1*d*).
Vol. II. Stability and Control, Structures, Seaplanes, Engines, etc. 50*s.* (51*s.* 1*d.*)
1937 Vol. I. Aerodynamics General, Performance, Airscrews, Flutter and Spinning. 40*s.* (41*s.* 1*d.*)
Vol. II. Stability and Control, Structures, Seaplanes, Engines, etc. 60*s.* (61*s.* 1*d.*)
1938 Vol. I. Aerodynamics General, Performance, Airscrews. 50*s.* (51*s.* 1*d.*)
Vol. II. Stability and Control, Flutter, Structures, Seaplanes, Wind Tunnels, Materials. 30*s.* (31*s.* 1*d.*)
1939 Vol. I. Aerodynamics General, Performance, Airscrews, Engines. 50*s.* (51*s.* 1*d.*)
Vol. II. Stability and Control, Flutter and Vibration, Instruments, Structures, Seaplanes, etc. 63*s.* (64*s.* 2*d.*)
1940 Aero and Hydrodynamics, Aerofoils, Airscrews, Engines, Flutter, Icing, Stability and Control, Structures, and a miscellaneous section. 50*s.* (51*s.* 1*d.*)
1941 Aero and Hydrodynamics, Aerofoils, Airscrews, Engines, Flutter, Stability and Control, Structures. 63*s.* (64*s.* 2*d.*)
1942 Vol. I. Aero and Hydrodynamics, Aerofoils, Airscrews, Engines. 75*s.* (76*s.* 3*d.*)
Vol. II. Noise, Parachutes, Stability and Control, Structures, Vibration, Wind Tunnels. 47*s.* 6*d.* (48*s.* 7*d.*)
1943 Vol. I. Aerodynamics, Aerofoils, Airscrews, 80*s.* (81*s.* 4*d.*)
Vol. II. Engines, Flutter, Materials, Parachutes, Performance, Stability and Control, Structures. 90*s.* (91*s.* 6*d.*)
1944 Vol. I. Aero and Hydrodynamics, Aerofoils, Aircraft, Airscrews, Controls. 84*s.* (85*s.* 8*d.*)
Vol. II. Flutter and Vibration, Materials, Miscellaneous, Navigation, Parachutes, Performance, Plates, and Panels, Stability, Structures, Test Equipment, Wind Tunnels. 84*s.* (85*s.* 8*d.*)

ANNUAL REPORTS OF THE AERONAUTICAL RESEARCH COUNCIL—

1933–34	1*s.* 6*d.* (1*s.* 8*d.*)	1937	2*s.* (2*s.* 2*d.*)
1934–35	1*s.* 6*d.* (1*s.* 8*d.*)	1938	1*s.* 6*d.* (1*s.* 8*d.*)
April 1, 1935 to Dec. 31, 1936.	4*s.* (4*s.* 4*d.*)	1939–48	3*s.* (3*s.* 2*d.*)

INDEX TO ALL REPORTS AND MEMORANDA PUBLISHED IN THE ANNUAL TECHNICAL REPORTS, AND SEPARATELY—

April, 1950 - - - - - R. & M. No. 2600. 2*s.* 6*d.* (2*s.* 7½*d.*)

AUTHOR INDEX TO ALL REPORTS AND MEMORANDA OF THE AERONAUTICAL RESEARCH COUNCIL—

1909–1949 - - - - - R. & M. No. 2570. 15*s.* (15*s.* 3*d.*)

INDEXES TO THE TECHNICAL REPORTS OF THE AERONAUTICAL RESEARCH COUNCIL—

December 1, 1936 — June 30, 1939.	R. & M. No. 1850.	1*s.* 3*d.* (1*s.* 4½*d.*)
July 1, 1939 — June 30, 1945.	R. & M. No. 1950.	1*s.* (1*s.* 1½*d.*)
July 1, 1945 — June 30, 1946.	R. & M. No. 2050.	1*s.* (1*s.* 1½*d.*)
July 1, 1946 — December 31, 1946.	R. & M. No. 2150.	1*s.* 3*d.* (1*s.* 4½*d.*)
January 1, 1947 — June 30, 1947.	R. & M. No. 2250.	1*s.* 3*d.* (1*s.* 4½*d.*)
July, 1951 - - - -	R. & M. No. 2350.	1*s.* 9*d.* (1*s.* 10½*d.*)

Prices in brackets include postage.

Obtainable from

HER MAJESTY'S STATIONERY OFFICE

York House, Kingsway, London W.C.2 ; 423 Oxford Street, London W.1 (Post Orders : P.O. Box No. 569, London S.E.1) ; 13A Castle Street, Edinburgh 2 ; 39 King Street, Manchester 2 ; 2 Edmund Street, Birmingham 3 ; 109 St. Mary Street, Cardiff ; Tower Lane, Bristol 1 ; 80 Chichester Street, Belfast OR THROUGH ANY BOOKSELLER

S.O. Code No. 23-2941

R. & M. No. 2941